

This discussion paper is/has been under review for the journal *Atmospheric Chemistry and Physics (ACP)*. Please refer to the corresponding final paper in *ACP* if available.

**Observational study
of aerosol
hygroscopic growth
factors**

X. L. Pan et al.

Observational study of aerosol hygroscopic growth factors over rural area near Beijing mega-city

X. L. Pan^{1,2,3}, P. Yan¹, J. Tang¹, J. Z. Ma¹, Z. F. Wang², and A. Gbaguidi²

¹Chinese Academy of Meteorological Science, China Meteorological Administration, Beijing, China

²Nansen-Zhu International Research Centre, Institute of Atmospheric Physics, Chinese Academy of Sciences, Beijing, China

³Graduate University of Chinese Academy of Sciences, Beijing, China

Received: 25 December 2008 – Accepted: 12 January 2009 – Published: 25 February 2009

Correspondence to: J. Tang (tangj@cams.cma.gov.cn)

Published by Copernicus Publications on behalf of the European Geosciences Union.

Title Page

Abstract

Introduction

Conclusions

References

Tables

Figures

⏪

⏩

◀

▶

Back

Close

Full Screen / Esc

Printer-friendly Version

Interactive Discussion

Abstract

We investigated aerosol hygroscopic growth property and its influence on scattering coefficient using M9003 nephelometers in coupling with a relative humidity controlled inlet system at a rural site near Beijing mega-city (Jingjintang) from 24th April to 15th May 2006. Inlet relative humidity was controlled in an increasing range of 40%–90% while the aerosol hygroscopic growth factor, $f(\text{RH}=80\%)$, varied in a range of 1.07–2.35 during the measurement. Estimated periodic mean values of aerosol hygroscopic growth factors are 1.27–1.34, 1.17–1.23, 1.55–1.59 and 2.33–2.48 for clean, dust, urban pollution and mixed pollution periods respectively. An examination of chemical composition of daily filter samples highlighted that aerosol hygroscopicity was generally enhanced with the increasing ratio of ammonium sulfate (AS) to organic matter (OMC). Furthermore, strong hygroscopic organic aerosols were observed on 11th ($f(\text{RH}=80\%)=2.23$) and 15th ($f(\text{RH}=80\%)=2.21$) of May with organic carbon proportions of $\text{PM}_{2.1}$ reaching 42.3% and 43.0% respectively. Back-trajectory analysis indicated that solar radiation and vertical convective movement along the air mass pathway might strongly influence the hygroscopic properties of organic matter.

1 Introduction

Aerosol hygroscopic growth with increasing relative humidity (RH) may lead to dramatic changes in its mass concentration, size distribution and corresponding optical properties (scattering coefficient, single scattering albedo, asymmetry factor etc.), which could enhance the cooling effect of aerosols in the atmosphere by directly scattering more light radiation (Carrico et al., 1998; Kotchenruther and Hobbs, 1998; Carrico et al., 2000; Randles et al., 2004), or change cloud microphysical properties (Crumevolle et al., 2008) by serving as cloud condensation nuclei (CCN) (Houghton et al., 2001). To precisely evaluate the direct radiative forcing, light scattering coefficient (σ_{sp}) of aerosol particles and its dependency on relative humidity (RH), defined as $f(\text{RH})=\sigma_{sp}$ (scanning

Observational study of aerosol hygroscopic growth factors

X. L. Pan et al.

Title Page

Abstract

Introduction

Conclusions

References

Tables

Figures

⏪

⏩

◀

▶

Back

Close

Full Screen / Esc

Printer-friendly Version

Interactive Discussion

**Observational study
of aerosol
hygroscopic growth
factors**

X. L. Pan et al.

Title Page

Abstract

Introduction

Conclusions

References

Tables

Figures

⏪

⏩

◀

▶

Back

Close

Full Screen / Esc

Printer-friendly Version

Interactive Discussion

RH)/ σ_{sp} (dry), have been investigated for decades through Integrating Nephelometers equipped with humidity control devices in clean background regions, marine boundary layers, rural and urban areas (Kotchenruther et al., 1999; Malm and Day, 2001; Malm et al., 2005; Carrico et al., 2003; Kim et al., 2006; Magi and Hobbs, 2003). Previous studies reported that different types of aerosol particles usually have distinct hygroscopic growth properties (Kim et al., 2006; Cruz and Pandis, 2000). Hand and Malm (2006) indicated that the scattering coefficients of $(\text{NH}_4)_2\text{SO}_4$ and $(\text{NH}_4)\text{HSO}_4$ aerosols could be enhanced by a factor of three when relative humidity is over 85%. Dust particles, dominant in coarse mode, are mostly insoluble with $f(\text{RH}=80\%)$ smaller than 1.1 (Li-Jones et al., 1998), but they could also be hygroscopic when coated by sulfate or other soluble inorganic aerosols during transportation (Shi et al., 2008; Perry et al., 2004). During the period of Aerosol Characterization Experiment (ACE-Asia), dust particle's hygroscopic factor of $f(\text{RH}=80\%)=1.25$ was observed in Ron Brown cruise (Carrico et al., 2003), and even as high as 2.0 in Korea (Kim et al., 2006). Combustion-emitted smoke organic matters and photochemically formed organic compounds, accounting for a significant proportion of particulate aerosols, could be hygroscopic or hydrophobic depending on the types of organics and their oxidation status in the atmosphere. Studies (Carrico et al., 2005) conducted in the Yosemite National Park indicated an inverse relationship between the organic carbon mass fraction of $\text{PM}_{2.5}$ and the hygroscopicity of aerosols. Researches carried out by Malm et al. (2005) in the same location showed that $f(85\%<\text{RH}<90\%)$ decreased from 2.0 to <1.2 as the ratio of organic carbon mass to $(\text{NH}_4)_2\text{SO}_4$ increased from 0.57 to 11.15. Nevertheless, inorganic aerosols' hygroscopicity enhanced by organic acids were also observed in some studies (Choi and Chan, 2002; Cruz and Pandis, 2000). Therefore, following the great temporal and spatial variations of aerosols' hygroscopic growth properties, in situ and laboratory investigations are needed.

In the past two decades, the rapid economy growth triggered China's annual GDP reaching over 9%, growing number of megacities (population over 10 millions), and increasing number of private cars (<http://www.stats.gov.cn/>), and consequently, the coun-

**Observational study
of aerosol
hygroscopic growth
factors**

X. L. Pan et al.

Title Page

Abstract

Introduction

Conclusions

References

Tables

Figures

⏪

⏩

◀

▶

Back

Close

Full Screen / Esc

Printer-friendly Version

Interactive Discussion

try become an important source of pollutants and aerosols production. Aerosols mass concentrations and their optical properties must have changed to some extent. In such condition, providing insights into aerosols optical properties and its dependence on relative humidity in some Chinese key regions seems to be an important scientific issue to better understand the relationships between aerosols and climate. Previously, studies of Yan et al. (2008) at Shangdianzi (SDZ), a baseline air pollution monitoring station of North China, showed that the f (RH=80%) was 1.16 in clean air conditions and 1.34 during pollution episodes in winter time. Kim et al. (2006) obtained higher value of 2.75 during the ACE-Asia period. Experiment carried out in the Pearl River Delta (PRD) region (Liu et al., 2007) also indicated the urban pollutants aerosols hygroscopic growth factor f (RH=80%) of about 2.04 for Guangzhou.

The present analysis of the aerosol hygroscopic factors f (RH) over the rural area in near Beijing Mega-city is based on an observational experiment performed from 25th April to 15th May, 2006. The main purpose of this study is to examine the effect of aerosol chemical composition on the hygroscopic growth and its scattering properties. The relationship between the aerosols hygroscopicity and the air mass back-trajectory pathway will be also discussed.

2 Observational experiment

2.1 Site description and meteorology

Measurements of the hygroscopic properties of aerosol scattering coefficient and aerosol sampling were conducted at Xin'An weather operational station in Baodi county (referred simply as Xin'An site, 39°44' N, 117°17' E, altitude: 6 m) located in the rural areas of Jing-Jin-Tang region (Fig. 1). Baodi is a major agricultural district of northern China, where rice and corn are cultivated. The principal human economical activities are farming and tree growing. The site which is about 85 km, 70 km and 105 km far from Beijing, Tianjin and Tangshan respectively, seems to be strongly under megacities air

pollution influence (seen Fig. 1). During the observation, meteorological condition was characterized by clear and sunny days, except for the floating dust event at approximately 1600LST (Local Standard Time) 30th April. Air temperature average of the experimental period was 16.1°, and relative humidity about 52.9%. The surface wind direction at the Xin'An site was dominated by NW wind and E wind, the wind speed less than 5 m/s. .

2.2 Instrumentation and method

Aerosol scattering coefficient (σ_{sp}) was measured with M9003 integrating nephelometer at 525 nm wavelength with light integrating angle 10°–170°. The measurement range of this instrument is 0–2000 Mm⁻¹ (1 Mm⁻¹ = 10⁻⁶ m⁻¹) with its lower detection limit of about 0.3 Mm⁻¹ (lower than one tenth of Rayleigh scattering of air molecules). The increase of scattering coefficients of aerosols as a function of relative humidity is represented by the ratio of aerosol scattering coefficient at conditioned relative humidity and that under the reference “dry” conditions (usually with RH less than 40%). This method was initially introduced by Covert et al. (1972). In measurement, relative humidity of the sampled air with reference nephelometer for “dry” measurement was controlled at RH below 40%, and the other one was operated at the RH scanning from 40% to 90% controlled with humidity control device (scanning humidifier). The structure of humidifier was similar with that used in NOAA/GMD (http://www.esrl.noaa.gov/gmd/aero/instrumentation/humid.html), It consisted in an internal water-vapor penetration membrane tube immersed in “deionized water bath” of the sheath pipe. The vapor was permeated to mix with sample air and the relative humidity of the air was modulated by controlling of the water temperature. The relative humidity and temperature of inflow air were measured with a build-in sensor in the nephelometer. Fig.2 presents the structure of the humidifier.

The aerosol hygroscopic growth factor is determined by the formula:

$$f(\text{RH} = 80\%) = \sigma_{sp}(\text{RH} = 80\%) / \sigma_{sp}(\text{RH} < 40\%) \quad (1)$$

Observational study of aerosol hygroscopic growth factors

X. L. Pan et al.

Title Page

Abstract

Introduction

Conclusions

References

Tables

Figures

⏪

⏩

◀

▶

Back

Close

Full Screen / Esc

Printer-friendly Version

Interactive Discussion



Obtained data are then fit into the following empirical equation.

$$f(\text{RH}) = 1 + a(\text{RH}/100)^b \quad (2)$$

During the observation period, the nephelometers were calibrated with the zero gas (dry filtered air) every 24 h, and with the standard calibration gas (R134a) every 7 days. The data were automatically recorded every 5 minutes. Additional test on humidity sensor and dry scattering measurements were performed. The comparison of humidity sensors of two nephelometers with HMP41/45 Visala humidity indicator showed in good agreement with the difference less than 3%. To correct the systematic signal bias of two nephelometers for aerosol scattering coefficient measurement, the normalized procedure reported by Day and Malm (2000) was conducted to make the ratio of scattering coefficients equal to one when RH was lower than 35%.

2.3 Aerosol sampling and chemical analysis

Aerosol particles were collected by using two sets of Anderson size-segregated impactors (KA2000). The cut-off size ranges are: $>11 \mu\text{m}$, $11\text{--}7 \mu\text{m}$, $7\text{--}4.7 \mu\text{m}$, $4.7\text{--}3.3 \mu\text{m}$, $3.3\text{--}2.1 \mu\text{m}$, $2.1\text{--}1.1 \mu\text{m}$, $1.1\text{--}0.65 \mu\text{m}$, $0.65\text{--}0.43 \mu\text{m}$, and $<0.43 \mu\text{m}$, respectively. Teflon membranes were used as impaction substrates for the top eight stages, and Zeflour membranes (Pall Corporation) were for the backup filter (the bottom stage). Organic carbon matters were sampled with Quartz membranes (Whatman QMA). The mass flow controller was used to maintain a stable flow rate at 28.3 L/min during the sampling period, and the flow rate check was performed with a dry gas rotometer before and after each sampling cycle. The sampling generally started at 08:30 LST, and sampling intervals were more than 22 h. The inlet height was 2.5 m above ground level. The membranes containing aerosol samples were refrigerated at a temperature below -4° , and sent to the laboratory in Beijing for mass and chemical analysis. Teflon filter samples were continually collected from 25th April to 15th May 2006, whereas, the corresponding Quartz filter collections were performed at 3rd, 4th, 10th, 11th, 12th, 13th, 14, and 15th.

Observational study of aerosol hygroscopic growth factors

X. L. Pan et al.

Title Page

Abstract

Introduction

Conclusions

References

Tables

Figures

⏪

⏩

◀

▶

Back

Close

Full Screen / Esc

Printer-friendly Version

Interactive Discussion

**Observational study
of aerosol
hygroscopic growth
factors**

X. L. Pan et al.

Title Page

Abstract

Introduction

Conclusions

References

Tables

Figures

◀

▶

◀

▶

Back

Close

Full Screen / Esc

Printer-friendly Version

Interactive Discussion

Aerosol mass concentrations were determined by means of weighting filters with Satorius microbalance (precision: $10\ \mu\text{g}$) before and after sample collection in the glove box. The filters were balanced in the glove box at a stable relative humidity ($40\pm 2\%$) and temperature ($20\pm 1^\circ$) environment for about 72 h prior to weighting process. Each membrane was weighted three times in 2 days according to the standard procedure, and the difference of gross mass of the filter weighted each time was less than $50\ \mu\text{g}$.

Inorganic anions (F^- , Cl^- , NO_3^- , SO_4^{2-}) was analyzed with Dionex 500 ion chromatography (IC), and cations (NH_4^+ , K^+ , Na^+ , Ca^{2+} , Mg^{2+}) with HITACHI 180-70 flame atomic absorption spectrophotometer (FAAS) at the Key Laboratory of Atmospheric Chemistry, China Meteorological Administration (CMA). Organic carbon (OC) was analyzed using thermal/optical carbon analyzer (Sunset Lab) at the Center of Environment, Peking University, and the precision and detection limits (LDC) are 10% and $2\ \mu\text{g cm}^{-2}$, respectively. The Quartz filters was pre-treated at temperature of 600° for 4 hours before sampling, and the sampled filters were stored in a refrigerator at -20° at the site before there were sent to the laboratory for analysis.

3 Results and discussion

3.1 Aerosol mass concentrations and chemical characteristics

During spring over Northern China, aerosol chemical properties are rather complex because of the mixture of different sources including transportation of heavy air pollution from urbanization and industrial activities, desert dust particles from frequent dust events, and local emitted plant organic compounds during vegetal “greening”. Statistic summary of aerosol mass concentrations, water soluble inorganic ion species, organic carbon are illustrated in Table 1. The average concentrations of fine particles ($\text{PM}_{2.1}$, particle matter which pass through a size selective inlet with a 50% efficiency cut-off at 2.1 aerodynamic diameter) and coarse particles (PM_{11}) were $81.01\ \mu\text{g}\cdot\text{m}^{-3}$ and $214.32\ \mu\text{g}\cdot\text{m}^{-3}$ with standard deviations of $32.76\ \mu\text{g}\cdot\text{m}^{-3}$ and $125.34\ \mu\text{g}\cdot\text{m}^{-3}$, respec-

**Observational study
of aerosol
hygroscopic growth
factors**

X. L. Pan et al.

Title Page

Abstract

Introduction

Conclusions

References

Tables

Figures

⏪

⏩

◀

▶

Back

Close

Full Screen / Esc

Printer-friendly Version

Interactive Discussion

tively. The concentration of PM_{11} exceeded the National Ambient Air Quality Secondary Standard of China (daily average $150 \mu\text{g}\cdot\text{m}^{-3}$), and the concentration of $PM_{2.1}$ is even over 2 times as high as the limit value of Primary Standard (daily average $35 \mu\text{g}\cdot\text{m}^{-3}$) of US Environmental Protection Agency. The maximum of particle mass concentration took place in the dust episode (on 30th April, according to the meteorological records) with the daily average PM_{11} concentration of $693.3 \mu\text{g}\cdot\text{m}^{-3}$ and $PM_{2.1}$ of $128.2 \mu\text{g}\cdot\text{m}^{-3}$. Aerosol mass concentrations are more similar with the experiments carried out in the suburban area of Beijing (Sun et al., 2004; Wang et al., 2005).

The mass concentration of soluble inorganic ions (SO_4^{2-} , NH_4^+ , NO_3^- , Ca^{2+} , Mg^{2+} , Na^+ , K^+ , Cl^-) and OC are listed in the Table 1. For the whole observation period, organic carbon accounts for the largest percentage of aerosol masses both in the $PM_{2.1}$ and PM_{11} with mean values (standard deviation) of $29.84 (9.02) \mu\text{g}\cdot\text{m}^{-3}$ and $61.44 (16.65) \mu\text{g}\cdot\text{m}^{-3}$. Many previous observation studies showed an approximately same OC concentration level at the near study site (Jing-Jin-Tang). For instance, He (2001) reported that organic carbon was most abundant species of the total $PM_{2.5}$ mass (annual mean value of $29.1 \mu\text{g}\cdot\text{m}^{-3}$) in the Beijing urban site, ranging from 17.9% to 25.7%. OC annual average of $20.04(12.07) \mu\text{g}\cdot\text{m}^{-3}$ in $PM_{2.5}$ was also observed (Duan et al., 2004) in the background site of Beijing surrounding areas, and the high OC concentration was mostly in connection with urban residential activities (Yang et al., 2005) and biomass burning (Duan et al., 2004). In $PM_{2.1}$ category, mass concentration of soluble SO_4^{2-} ion was $11.5(7.6) \mu\text{g}\cdot\text{m}^{-3}$, followed by NO_3^- and NH_4^+ ions with value of $6.05(4.52) \mu\text{g}\cdot\text{m}^{-3}$ and $4.02(3.17) \mu\text{g}\cdot\text{m}^{-3}$. This indicated anthropogenic urban pollution influences during the observation period. In the PM_{11} , soluble Ca^{2+} ion makes up the second largest proportion of aerosol masses, which might be related to flowing dirt during the springtime generally featured by low ambient relative humidity and strong wind.

3.2 Aerosols hygroscopic growth

3.2.1 Observation periods distinction

All the $f(\text{RH})$ displayed a similar appearance in the general shape of the hygroscopic growth (monotonic increasing) in spite of significant scattering of data points and wide range of deliquescent RH, and temporal variation of $f(\text{RH}=80\%)$ (Fig. 3). In the plot, the high variations should be closely related to the unique dominant aerosols types at Xin'An site. We therefore categorized aerosols into four different groups according to air mass concentration and chemical compositions (Table 2). Also, 48-h air mass back-trajectories were used by means of the Hybrid Single-particle Lagrangian Integrated Trajectory (HYSPPLIT) model (Draxler and Hess, 1998). Meteorological fields with 6-hour time interval (formatted as FNL) used in the back-trajectory analysis were obtained from US National Centers for Environmental Prediction (NECP). The back trajectory starting geographical position was located at Xin'An site with starting altitude of 100 m. The dissociation of aerosols concentrations periodicity can be described as follows:

1. Detect periods influenced by pronounced dust aerosols in accordance with observational records and 3 h meteorological information (Provided by China Meteorological Administration, CMA). The floating dust episode occurred in the afternoon of 30 April (approximately 17:00 LST) while the local visibility was less than 1 km. While mass concentration of coarse particles (PM_{11}) reached $693.25 \mu\text{g}\cdot\text{m}^{-3}$, the mass concentration of fine particles ($\text{PM}_{2.1}$) was about $128.22 \mu\text{g}\cdot\text{m}^{-3}$, accounting for only 18.5% of the total mass concentration. This is supported by observation performed by Wang et al. (2007) of which the mass concentration of TSP was about $419\text{--}879 \mu\text{g}\cdot\text{m}^{-3}$, with $\text{PM}_{2.5}$ of $156\text{--}286 \mu\text{g}\cdot\text{m}^{-3}$ during the dust storm period in Beijing, 2004. Air mass 48 h back-trajectories also indicated that strong wind from northwestern China was oriented towards Mongolian Plateau and Hunshandake desert in north of Beijing.

Observational study of aerosol hygroscopic growth factors

X. L. Pan et al.

Title Page

Abstract

Introduction

Conclusions

References

Tables

Figures

⏪

⏩

◀

▶

Back

Close

Full Screen / Esc

Printer-friendly Version

Interactive Discussion

**Observational study
of aerosol
hygroscopic growth
factors**

X. L. Pan et al.

Title Page

Abstract

Introduction

Conclusions

References

Tables

Figures

⏪

⏩

◀

▶

Back

Close

Full Screen / Esc

Printer-friendly Version

Interactive Discussion

2. Select the periods where mass concentration of fine particles ($PM_{2.1}$) are less than $50 \mu\text{g}\cdot\text{m}^{-3}$ as “clean periods”, and use this value as delimitation of clean-to-pollution on the ground where the value is approximately equivalent to Air Pollution Index (<http://www.mep.gov.cn/>) of about 50 (indication of “good” air quality in China). On 5th, 10th and 13th and 14th May, the daily average mass concentration of $PM_{2.1}$ were $39.2 \mu\text{g}\cdot\text{m}^{-3}$, $42.0 \mu\text{g}\cdot\text{m}^{-3}$, $42.7 \mu\text{g}\cdot\text{m}^{-3}$ and $49.8 \mu\text{g}\cdot\text{m}^{-3}$, those of PM_{11} were $141.1 \mu\text{g}\cdot\text{m}^{-3}$, $144.8 \mu\text{g}\cdot\text{m}^{-3}$, $157.7 \mu\text{g}\cdot\text{m}^{-3}$ and $145.6 \mu\text{g}\cdot\text{m}^{-3}$ respectively, generally lower than the National Ambient Air Quality Secondary Standard of China (daily average $150 \mu\text{g}\cdot\text{m}^{-3}$).

3. Consider the periods where particles ($PM_{2.1}$) are over $50 \mu\text{g}\cdot\text{m}^{-3}$ as influenced by urban pollution, because the site is located in the center of three pollution source areas, Beijing, Tianjin and Tangshan, urban emitted anthropogenic pollutants might be easily transported to the observation site with sea-land breezes and northwest wind. As shown on Fig. 3, on 11th and 15th May, aerosol hygroscopic growth factors $f(\text{RH}=80\%)$ were apparently higher than that of other periods, we defined this phase as “mixed pollution type” discussed in Sect. 3.2.5. Dissociated other periods were considered as “urban pollution” featured by relative high mean mass concentrations of SO_4^{2-} , NO_3^- ions about $13.1 \mu\text{g}\cdot\text{m}^{-3}$ and $7.2 \mu\text{g}\cdot\text{m}^{-3}$ respectively. Back-trajectories analysis showed that air mass mostly come from pollutant areas of southern regions such as Tianjin, Shijiazhuang, and eastern Tangshan towards Xin’An site. Detailed analysis of the periods allows quantifying the variation of aerosols hygroscopic factors.

3.2.2 Clean period

During the clean days, aerosol hygroscopic growth features, $f(\text{RH}=80\%)$ showed large temporal variations (Fig. 3) with averaged measured of 1.31, corresponding to about 10% higher than ($f(\text{RH}=80\%)=1.16$) indicated by Yan et al. (2008) for an other rural site (100 km northeast far from Xin’An site) of north Beijing in winter, and about 11%

and 29% lower than the results ($f(\text{RH}=80\%)=1.42$) reported by Koloutsou-Vakakis et al. (2001) for the northern hemisphere continental site (Bondville, Illinois, US) and ($f(\text{RH}=80\%)=1.40$) measured by Carrico et al. (2000) in the clean air conditions in Sagres (Portugal, ACE-2) respectively. The values above were derived from the fitting equations provided by authors. In Bondville site, local high sulfate burden and SO_2 concentration, reported by Charlson et al. (1991) and Harris and Kahl (1994) might be the possible contributions to relatively higher $f(\text{RH}=80\%)$, while Studies of Yan et al. were performed in the baseline air monitoring station of Northern China, where geographical environment within 30 km radius distance was characterized by rolling hills farmland, orchard and forests with lower pollutants concentrations. Besides, the differences of dominant aerosol composition in winter and in spring might also be the possible reason for this disparity. Note that the hygroscopic growth factor $f(\text{RH})$ depends on size range of measured inlet aerosol particles and wavelength of nephelometer optics. For the present study, we measured scattering coefficient and its hygroscopicity of total suspended aerosols, whereas the above authors obtained values of $f(\text{RH}=80\%)$ were determined under aerosol diameter less than $10\mu\text{m}$ condition. These factors may be an explanation of such discrepancy in the results.

3.2.3 Dust episode

Measured hygroscopic growth factor $f(\text{RH}=80\%)$ was 1.20 in dust episode. This value seemed to be close to the results obtained by Carrico et al. (2003), of which aerosol hygroscopic factors $f(\text{RH}=82.5\%)$ were 1.18 and 1.39 for particles size less than $10\mu\text{m}$ and $1\mu\text{m}$ respectively in East Asia (ACE-Asia) during dust dominant period. Observational experiment performed by Kim et al. (2006) in Kosan (South Korea) indicated aerosol $f(\text{RH}=85\%)=1.73\text{--}2.20$ during dust episode. These differences might be resulted from the mixing effect of dust particles with other inorganic materials during transportation. This is supported by many previous studies on dust particles over marine (Yamato and Tanaka, 1994; Zhang et al., 2003) or urban areas (Wang et al., 2007; Zhang and Iwasaka, 1999) of which the authors demonstrated that the mixing

**Observational study
of aerosol
hygroscopic growth
factors**

X. L. Pan et al.

Title Page

Abstract

Introduction

Conclusions

References

Tables

Figures

⏪

⏩

◀

▶

Back

Close

Full Screen / Esc

Printer-friendly Version

Interactive Discussion

of sulfate, nitrate, and coarse calcium in dust particles could substantially enhance the hygroscopicity. Coarse calcium dust particles with nitrate-containing could appear in aqueous phase even at 15% RH (Shi et al., 2008).

3.2.4 Urban pollution period

5 Under the urban anthropogenic pollutants dominance condition, humidograms showed little evidence of deliquescence but monotonic changes in scattering coefficient with increasing control RH (Fig. 4). Measured aerosol hygroscopic growth factor $f(\text{RH}=80\%)$ is 1.57, about 6% greater than the results ($f(\text{RH}=80\%)=1.48$) for pollution episodes obtained by Yan et al. (2008) in the urban site of Beijing city. Mean mass concentration of $\text{PM}_{2.1}$ is $87.9 \mu\text{g}\cdot\text{m}^{-3}$ two times higher than the value of “clean” periods, while averaged mass concentrations of SO_4^{2-} , NO_3^- , NH_4^+ ions in $\text{PM}_{2.1}$ are respectively 14.51 $\mu\text{g}\cdot\text{m}^{-3}$, 8.06 $\mu\text{g}\cdot\text{m}^{-3}$ and 5.02 $\mu\text{g}\cdot\text{m}^{-3}$, obviously higher than those obtained in clean periods (4.63 $\mu\text{g}\cdot\text{m}^{-3}$, 1.78 $\mu\text{g}\cdot\text{m}^{-3}$ and 1.57 $\mu\text{g}\cdot\text{m}^{-3}$). Kim et al. (2006) reported approximately same $f(\text{RH}=80\%)=1.55\text{--}1.77$ for pollution (from Korea industrial area) episode in Gosan regional background site. ACE-2, experiments conducted by Carri-
10 rico et al. (2000) in Sagres showed that $f(\text{RH}=80\%)$ value of 1.40 for anthropogenic pollutant (PM_{10}) from Europe, about 11% lower than measured results in the present study. This might be related to the differences of physico-chemical properties of regional scale aerosols (Allen et al., 1999). Many other studies (Table 3) indicated more
15 hygroscopic properties of urban aerosols, 2.04 ± 0.28 in PRD region (Liu et al., 2007), 1.7–2.0 in Yangtze delta region (Xu et al., 2002) and $1.81\pm 0.37\sim 2.30\pm 0.24$ in the flight over east coast of United States (Kotchenruther et al., 1999). Among these studies, Liu et al. (2007) determined the urban pollution periods in terms of air mass back trajectories and Kotchenruther et al. (1999) classified the periods by airflow patterns, and they
20 did not provide specific information of aerosol mass concentrations. It seems therefore difficult to provide wider insights into such results gap.
25

Observational study of aerosol hygroscopic growth factors

X. L. Pan et al.

Title Page

Abstract

Introduction

Conclusions

References

Tables

Figures

⏪

⏩

◀

▶

Back

Close

Full Screen / Esc

Printer-friendly Version

Interactive Discussion

3.2.5 Mixed Pollution episode

Under significant influence of urban pollution, we distinguished two main episodes (11th and 15th May respectively) of which aerosols hydrophilicity and its effects on scattering coefficient were relatively higher. Measured hygroscopic growth factor f (RH=80%) reached 2.33–2.48, close to the value of mixed aerosols (marine and urban aerosols) in the PRD region (Liu et al., 2007). Analysis of water-soluble inorganic ions highlighted drastic increment of Na^+ mass concentration in $\text{PM}_{2.1}$ from 11th to 15th May with mean value of about $3.78 \mu\text{g}\cdot\text{m}^{-3}$ (standard deviation of 1.21), higher than that (averagely $1.10 \mu\text{g}\cdot\text{m}^{-3}$) of unmixed pollution periods, suggesting evidence of marine aerosols impact (Chan et al., 1997; McInnes et al., 1996). Daily average mass concentration of SO_4^{2-} at 11 and 15 May are $4.32 \mu\text{g}\cdot\text{m}^{-3}$ and $9.26 \mu\text{g}\cdot\text{m}^{-3}$ respectively. Analysis of back trajectory showed air masses direction oriented from Tianjin-Tangshan (Fig. 6). In addition, organic matters proportions in $\text{PM}_{2.1}$ increased of about 42.3% and 43.0% on 11th and 15th May respectively, 50% and 61% higher than mean values of unmixed urban pollution periods. Biomass burning may be the most probable source of suspended organic particles in the atmosphere (Duan et al., 2004), however, we do not find any signs of fire events around the Xin'An site from MODIS active fire data (provided by the MODIS Rapid Response System <http://maps.geog.umd.edu/firms/>) during that time. Then, the two episodes might be influenced by a complex “mixed aerosols” occurrence of involving urban pollution, marine and large portion of organic matters.

3.3 Aerosol hygroscopic growth function

Aerosols hygroscopic growth trends in dust, clean, urban pollution and mixed periods are shown in Fig. 4. Large variations of aerosols water absorbing ability appear among different dominant aerosols types. Aerosols hygroscopic growth functions are obtained from Eq. (1), and used for monotonic growth illustration (Carrico et al., 2003; Kotchenruther and Hobbs, 1998; Kotchenruther et al., 1999; Liu et al., 2007; Magi and Hobbs, 2003). The parameters of (a) and (b) are described in Table 4. Both (a) and (b) seem to

Observational study of aerosol hygroscopic growth factors

X. L. Pan et al.

Title Page

Abstract

Introduction

Conclusions

References

Tables

Figures

⏪

⏩

◀

▶

Back

Close

Full Screen / Esc

Printer-friendly Version

Interactive Discussion

be undergone a sharply increase from dust particles ($a=0.64$, $b=5.17$) to mixed aerosol types ($a=7.68$, $b=7.62$).

3.4 Influence of organic matters on aerosol hygroscopicity

Aerosol mass concentrations and proportions of SO_4^{2-} , NO_3^- , NH_4^+ , and organic carbon in $\text{PM}_{2.1}$ are summarized in Table 5. To better characterize the hygroscopic properties of aerosols, the ratio of organic carbon matters (OMC)/ammonium sulfate (AS) (Malm et al., 2005) is estimated, ammonium sulfate and organic carbon matters are derived from the equations: $\text{AS}=0.944[\text{NH}_4^+]+1.02[\text{SO}_4^{2-}]$ and $\text{OMC}=1.4[\text{OC}]$ (Malm and Day, 2001). Figure 5 describes the relationship between OMC/AS and $f(\text{RH}=80\%)$. Except the period of “Mixed pollution”, the OMC/AS seems to be inversely correlated to $f(\text{RH}=80\%)$: an increase of the ratio increases (from 1.58 to 9.87) is associated with a decrease of $f(\text{RH}=80\%)$. The proportions of SO_4^{2-} , NO_3^- and NH_4^+ in $\text{PM}_{2.1}$ also display same systematically trends (Fig. 5). This indicates that water soluble inorganic ions are key factors directly correlated to aerosols water absorbing abilities as reported by (Malm et al., 2005; Virkkula et al., 1999). Organic matters serve therefore as hydrophobic compounds in aerosol particles chemical structure. However, different trends are obtained in mixed pollution periods. Proportions of OC in $\text{PM}_{2.1}$ are 40.0%, 43.0% for 11th and 15th May respectively, as much as two time of mean value (26.7%) of unmixed urban pollution periods (3rd, 4th, 12th May), while the aerosol hygroscopic growth factor increases by 46.0% associated with averaged $f(\text{RH}=80\%)=2.22$. The existence of water-soluble organic compounds in the aerosols seems to be strongly probable in such condition as suggested in many previous studies (Cruz and Pandis, 2000; Choi and Chan, 2002).

Figure 6 displays 48h Back-trajectory of air masses during pollution episodes (3rd, 4th, 11th, 12th and 15th May). It seems obvious that air masses on 11th May from remote areas of central Inner Mongolia province transiting over Tangshan and Tianjin as well as air masses on 15th May from Shanxi province, transiting over Taiyuan, Zhengzhou and Tianjin, may govern pollutants transport towards study site. During

Observational study of aerosol hygroscopic growth factors

X. L. Pan et al.

Title Page

Abstract

Introduction

Conclusions

References

Tables

Figures

◀

▶

◀

▶

Back

Close

Full Screen / Esc

Printer-friendly Version

Interactive Discussion



other pollution episodes, air masses are mostly from eastern China. Under the influence of microclimate and land vegetable coverage, the diversification of organic aerosol types from east (red dot shaded region in Fig. 6) and central part (blue dot shaded region in Fig. 6) of China might be an explanation of the discrepancies detected in hygroscopic properties. Furthermore, since aerosols physico-chemical properties and mixing type may be very likely undergone changes during transportation, meteorological parameters (solar radiation and mixing height) are specifically analyzed in pollution periods. Figure 7a shows the temporal and spatial variation of mixing height along the air masses pathways. The mixing height is about 3000 m at 14:00 LST on 15th May, and 1720 m on 11th May. This indicates strong vertical convection conditions in the boundary layer, favorable to mixing and chemical processes of local emitted and transported aerosols. The variations of solar radiation, susceptible to influence organic carbon photochemical reactions, are illustrated in the Fig. 7b. Three mostly strong solar radiation values: 871.5 Wm^{-2} , 812.1 Wm^{-2} and 655.7 Wm^{-2} are detected respectively on 15th, 3rd, and 11th May. Such condition may trigger the surface oxidation process of organic matters active function groups as well as corresponding water-absorbing ability (Chughtai et al., 1999; Charlson et al., 1992). Note that the $f(\text{RH}=80\%)$ on 3rd May is lower less than that of 11th and 15th May. This is probably related to the various sources of organic aerosols and the discrepancy in proportions of OC in $\text{PM}_{2.1}$ (daily average of 29.8%, 40.0% and 43.0% on 3rd, 11th and 15th May). However, further information on organic compounds still needed to insights into schematics of hygroscopicity and its influence on aerosols optical properties.

4 Conclusions

Aerosols hygroscopic growth experimental study over rural area (Jing-Jin-Tang) near Beijing mega-city through analysis of key meteorological parameters and aerosols chemical composition, results in smooth and monotonic growth features associated with increasing RH in most of observation periods. Experimental data allow catego-

Observational study of aerosol hygroscopic growth factors

X. L. Pan et al.

Title Page

Abstract

Introduction

Conclusions

References

Tables

Figures

⏪

⏩

◀

▶

Back

Close

Full Screen / Esc

Printer-friendly Version

Interactive Discussion

**Observational study
of aerosol
hygroscopic growth
factors**

X. L. Pan et al.

Title Page

Abstract

Introduction

Conclusions

References

Tables

Figures

◀

▶

◀

▶

Back

Close

Full Screen / Esc

Printer-friendly Version

Interactive Discussion

5 rizing pollution episodes in four different cases (clean, dust, urban pollution and mixed
pollution) in accordance with aerosols mass concentrations and chemical compositions
variations. (1) In the “clean” period, aerosols hygroscopic growth factor $f(\text{RH}=80\%)$ is
1.31, higher than the results report by Yan et al. (2008) in rural area of north China
10 (1.2), and lower than that of Koloutsou-Vakakis et al. (2001) measured in northern
hemisphere continental site (1.4–1.5) and Carrico et al. (2000) in Sagres Portugal
(1.69±0.16). (2) During the dust episode, $f(\text{RH}=80\%)=1.20$, far less than observa-
tional experiment result (1.73–2.20) obtained by Kim et al. (2006). The mixing effect
of dust particles with sulfate, nitrate and sea-salt aerosols may be a plausible expla-
15 nation of results divergence. (3) During urban pollutant phase, measured aerosol hy-
groscopic growth factor $f(\text{RH}=80\%)$ is 1.57, lower than values of 2.04±0.28 in south-
ern coast area of China, 1.7–2.0 in Yangtze delta region and 1.81±0.37–2.30±0.24 in
East coast of United States. (4) Marine and urban pollutant mixing aerosols present
greater water soluble ability with averaged $f(\text{RH}=85\%)$ of 2.40, slightly higher than
20 the value ($f(\text{RH}=80\%)=2.04$) reported in marine dominant air mass period (Carrico et
al., 2003), and that ($f(\text{RH}=80\%)=2.29±0.28$) in PRD coastal region during the urban-
marine mixed period (Liu et al., 2007). Analysis of back trajectory, solar radiation and
mixing height along the air masses pathways, indicates that organic aerosols types,
sources and the mixing process during the transportation play key roles in determining
25 particles hygroscopicity. The higher values of solar radiation also constitute an im-
portant favorable factor of water-soluble organic matters formation. Through present
experimental study, organic matters seem to importantly contribute to uncertainties of
aerosols hygroscopic properties as well as the variations of hygroscopic growth. Facing
this complexity, further experimental long-term study associated with specific modeling
analysis on the relationship between organic compounds and aerosols hygroscopicity
will be done in near future to thoroughly understand such physico-chemical process.

Acknowledgement. The authors thank Ding Guoan and the staff of the meteorological station
for giving us great help during the observations. Their works and professional dedication are
greatly respected and appreciated. This work is supported by the NSFC project (40675009)

and NSFC key project (40433008), and partly supported by the National Key Basic Research project (2006CB403701).

References

- Allen, G. A., Lawrence, J., and Koutrakis, P.: Field validation of a semi-continuous method for aerosol black carbon (aethalometer) and temporal patterns of summertime hourly black carbon measurements in southwestern PA, *Atmos. Environ.*, 33, 817–823, 1999.
- Carrico, C. M., Rood, M. J., and Ogren, J. A.: Aerosol light scattering properties at Cape Grim, Tasmania, during the First Aerosol Characterization Experiment (ACE 1), *J. Geophys. Res.*, 103, 16565–16574, 1998.
- Carrico, C. M., Rood, M. J., Ogren, J. A., Neususs, C., Wiedensohler, A., and Heintzenberg, J.: Aerosol Optical properties at Sagres, Portugal during ACE-2, *Tellus B*, 52, 694–715, 2000.
- Carrico, C. M., Kus, P., Rood, M. J., Quinn, P. K., and Bates, T. S.: Mixtures of pollution, dust, sea salt, and volcanic aerosol during ACE-Asia: Radiative properties as a function of relative humidity, *J. Geophys. Res.*, 108, 8650, doi:10.1029/2003jd003405, 2003.
- Carrico, C. M., Kreidenweis, S. M., Malm, W. C., Day, D. E., Lee, T., Carrillo, J., McMeeking, G. R., and Collett, J. L.: Hygroscopic growth behavior of a carbon-dominated aerosol in Yosemite National Park, *Atmos. Environ.*, 39, 1393–1404, 2005.
- Chan, Y. C., Simpson, R. W., McTainsh, G. H., Vowles, P. D., Cohen, D. D., and Bailey, G. M.: Characterisation of chemical species in PM_{2.5} and PM₁₀ aerosols in Brisbane, Australia, *Atmos. Environ.*, 31, 3773–3785, 1997.
- Charlson, R. J., Langner, J., Rodhe, H., Leovy, C. B., and Warren, S. G.: Perturbation of the northern hemisphere radiative balance by backscattering from anthropogenic sulfate aerosols*, *Tellus B*, 43, 152–163, 1991.
- Charlson, R. J., Schwartz, S. E., Hales, J. M., Cess, R. D., Coakley, J. A., Hansen, J. E., and Hofmann, D. J.: Climate Forcing by Anthropogenic Aerosols, *Science*, 255, 423–430, 1992.
- Choi, M. Y. and Chan, C. K.: The Effects of Organic Species on the Hygroscopic Behaviors of Inorganic Aerosols, *Environ. Sci. Technol.*, 36, 2422–2428, 2002.
- Chughtai, A. R., Williams, G. R., Atteya, M. M. O., Miller, N. J., and Smith, D. M.: Carbonaceous particle hydration, *Atmos. Environ.*, 33, 2679–2687, 1999.
- Covert, D. S., Charlson, R. J., and Ahlquist, N. C.: A study of the relationship of chemical

Observational study of aerosol hygroscopic growth factors

X. L. Pan et al.

Title Page

Abstract

Introduction

Conclusions

References

Tables

Figures

⏪

⏩

◀

▶

Back

Close

Full Screen / Esc

Printer-friendly Version

Interactive Discussion

- composition and humidity to light scattering by aerosols, *J. Appl. Meteorol.*, 11, 968–976, 1972.
- Crumeyrolle, S., Gomes, L., Tulet, P., Matsuki, A., Schwarzenboeck, A., and Crahan, K.: Increase of the aerosol hygroscopicity by cloud processing in a mesoscale convective system: a case study from the AMMA campaign, *Atmos. Chem. Phys.*, 8, 6907–6924, 2008, <http://www.atmos-chem-phys.net/8/6907/2008/>.
- Cruz, C. N. and Pandis, S. N.: Deliquescence and Hygroscopic Growth of Mixed Inorganic-Organic Atmospheric Aerosol, *Environ. Sci. Technol.*, 34, 4313–4319, 2000.
- Day, D. E., Malm, W. C., and Kreidenweis, S. M.: Aerosol light scattering measurements as a function of relative humidity, *J. Air Waste Manag. Assoc.*, 50, 710–716, 2000.
- Draxler, R. R. and Hess, G. D.: An overview of the HYSPLIT_4 modelling system for trajectories, dispersion, and deposition, *Australian Meteorological Magazine*, 47, 295–308, 1998.
- Duan, F., Liu, X., Yu, T., and Cachier, H.: Identification and estimate of biomass burning contribution to the urban aerosol organic carbon concentrations in Beijing, *Atmos. Environ.*, 38, 1275–1282, 2004.
- Hand, J. L. and Malm, W. C.: Review of the IMPROVE Equation for Estimating Ambient Light Extinction Coefficients-Final Report, 2006.
- Harris, J. M. and Kahl, J. D. W.: Analysis of 10-day isentropic flow patterns for Barrow, Alaska: 1985–992, *J. Geophys. Res.*, 99, 845–845, 1994.
- He, K., Yang, F., Ma, Y., Zhang, Q., Yao, X., Chan, C. K., Cadle, S., Chan, T., and Mulawa, P.: The characteristics of PM_{2.5} in Beijing, China, *Atmospheric Environment*, 35, 4959–4970, 2001.
- Kim, J., Yoon, S. C., Jefferson, A., and Kim, S. W.: Aerosol hygroscopic properties during Asian dust, pollution, and biomass burning episodes at Gosan, Korea in April 2001, *Atmos. Environ.*, 40, 1550–1560, 2006.
- Koloutsou-Vakakis, S., Carrico, C. M., Kus, P., Rood, M. J., Li, Z., Shrestha, R., Ogren, J. A., Chow, J. C., and Watson, J. G.: Aerosol properties at a midlatitude Northern Hemisphere continental site, *J. Geophys. Res.*, 106, 3019–3032, 2001.
- Kotchenruther, R. A. and Hobbs, P. V.: Humidification factors of aerosols from biomass burning in Brazil, *J. Geophys. Res.*, 103, 32081–32090, 1998.
- Kotchenruther, R. A., Hobbs, P. V., and Hegg, D. A.: Humidification factors for atmospheric aerosols off the mid-Atlantic coast of the United States, *J. Geophys. Res.*, 104, 2239–2252, 1999.

**Observational study
of aerosol
hygroscopic growth
factors**X. L. Pan et al.

[Title Page](#)[Abstract](#)[Introduction](#)[Conclusions](#)[References](#)[Tables](#)[Figures](#)[⏪](#)[⏩](#)[◀](#)[▶](#)[Back](#)[Close](#)[Full Screen / Esc](#)[Printer-friendly Version](#)[Interactive Discussion](#)

**Observational study
of aerosol
hygroscopic growth
factors**

X. L. Pan et al.

[Title Page](#)[Abstract](#)[Introduction](#)[Conclusions](#)[References](#)[Tables](#)[Figures](#)[⏪](#)[⏩](#)[◀](#)[▶](#)[Back](#)[Close](#)[Full Screen / Esc](#)[Printer-friendly Version](#)[Interactive Discussion](#)

Li-Jones, X., Maring, H. B., and Prospero, J. M.: Effect of relative humidity on light scattering by mineral dust aerosol as measured in the marine boundary layer over the tropical Atlantic Ocean, *J. Geophys. Res.*, 103(31), 31113–31121, 1998.

Liu, X., Cheng, Y., Zhang, Y., Jung, J., Sugimoto, N., Chang, S. Y., Kim, Y. J., Fan, S., and Zeng, L.: Influences of relative humidity and particle chemical composition on aerosol scattering properties during the 2006 PRD campaign, *Atmos. Environ.*, 42, 1525–1536, 2007.

Magi, B. I. and Hobbs, P. V.: Effects of humidity on aerosols in southern Africa during the biomass burning season, *J. Geophys. Res. Atmos.*, 108, 8495, doi:10.1029/2002jd002144, 2003.

Malm, W. C. and Day, D. E.: Estimates of aerosol species scattering characteristics as a function of relative humidity, *Atmos. Environ.*, 35, 2845–2860, 2001.

Malm, W. C., Day, D. E., Kreidenweis, S. M., Collett, J. L., Carrico, C., McMeeking, G., and Lee, T.: Hygroscopic properties of an organic-laden aerosol, *Atmos. Environ.*, 39, 4969–4982, 2005.

McInnes, L. M., Quinn, P. K., Covert, D. S., and Anderson, T. L.: Gravimetric analysis, ionic composition, and associated water mass of the marine aerosol, *Atmos. Environ.*, 30, 869–884, 1996.

Perry, K. D., Cliff, S. S., and Jimenez-Cruz, M. P.: Evidence for hygroscopic mineral dust particles from the Intercontinental Transport and Chemical Transformation Experiment, *J. Geophys. Res.*, 109, D23S28, doi:10.1029/2004jd004979, 2004.

Randles, C. A., Russell, L. M., and Ramaswamy, V.: Hygroscopic and optical properties of organic sea salt aerosol and consequences for climate forcing, *Geophys. Res. Lett.*, 31, L16108, doi:10.1029/2004gl020628, 2004.

Shi, Z., Zhang, D., Hayashi, M., Ogata, H., Ji, H., and Fujiie, W.: Influences of sulfate and nitrate on the hygroscopic behaviour of coarse dust particles, *Atmos. Environ.*, 42, 822–827, 2008.

Sun, Y., Zhuang, G., Wang, Y., Han, L., Guo, J., Dan, M., Zhang, W., Wang, Z., and Hao, Z.: The air-borne particulate pollution in Beijing – concentration, composition, distribution and sources, *Atmos. Environ.*, 38, 5991–6004, 2004.

Virkkula, A., Van Dingenen, R., Raes, F., and Hjorth, J.: Hygroscopic properties of aerosol formed by oxidation of limonene, alpha-pinene, and beta-pinene, *J. Geophys. Res.*, 104, 3569–3580, 1999.

Wang, Y., Zhuang, G., Tang, A., Yuan, H., Sun, Y., Chen, S., and Zheng, A.: The ion chemistry

**Observational study
of aerosol
hygroscopic growth
factors**

X. L. Pan et al.

[Title Page](#)[Abstract](#)[Introduction](#)[Conclusions](#)[References](#)[Tables](#)[Figures](#)[⏪](#)[⏩](#)[◀](#)[▶](#)[Back](#)[Close](#)[Full Screen / Esc](#)[Printer-friendly Version](#)[Interactive Discussion](#)

and the source of PM_{2.5} aerosol in Beijing, *Atmos. Environ.*, 39, 3771–3784, 2005.

Wang, Y., Zhuang, G., Tang, A., Zhang, W., Sun, Y., Wang, Z., and An, Z.: The evolution of chemical components of aerosols at five monitoring sites of China during dust storms, *Atmos. Environ.*, 41, 1091–1106, 2007.

5 Xu, J., Bergin, M. H., Yu, X., Liu, G., Zhao, J., Carrico, C. M., and Baumann, K.: Measurement of aerosol chemical, physical and radiative properties in the Yangtze delta region of China, *Atmos. Environ.*, 36, 161–173, 2002.

10 Yamato, M. and Tanaka, H.: Aircraft observations of aerosols in the free marine troposphere over the North Pacific Ocean: particle chemistry in relation to air mass origin, *J. Geophys. Res.*, 99, 5353–5377, 1994.

Yan, P., Pan, X. L., Tang, J., Zhou, X. J., and Zeng, L. M.: An experimental study on the influence of relative humidity on the atmospheric aerosol scattering coefficient at an urban site in Beijing, *Acta Meteorologica Sinica*, 6, 11–119, 2008.

15 Yang, F., He, K., Ye, B., Chen, X., Cha, L., Cadle, S. H., Chan, T., and Mulawa, P. A.: One-year record of organic and elemental carbon in fine particles in downtown Beijing and Shanghai, *Atmos. Chem. Phys.*, 5, 1449–1457, 2005.

Zhang, D. and Iwasaka, Y.: Nitrate and sulfate in individual Asian dust-storm particles in Beijing, China in Spring of 1995 and 1996, *Atmos. Environ.*, 33, 3213–3223, 1999.

20 Zhang, D., Iwasaka, Y., Shi, G., Zang, J., Matsuki, A., and Trochne, D.: Mixture state and size of Asian dust particles collected at southwestern Japan in spring 2000, *J. Geophys. Res.*, 108, 4760, doi:10.1029/2003jd003869, 2003.

Observational study of aerosol hygroscopic growth factors

X. L. Pan et al.

Table 1. Statistical summary of 24 h average aerosol species concentrations.

Variables ($\mu\text{g}\cdot\text{m}^{-3}$)	PM ₁₁ (Dp<11 μm)				PM _{2.1} (Dp<2.1 μm)				N
	mean	Std. Dev.	Maximum	Minimum	mean	Std. Dev.	Maximum	Minimum	
Mass concentration	214.32	125.34	693.25	119.5	81.01	32.76	178.2	38.65	21
NO ₃ ⁻	9.13	5.67	22.60	1.06	6.05	4.52	16.69	0.53	21
SO ₄ ²⁻	15.25	9.19	39.24	3.55	11.50	7.60	31.51	2.15	21
NH ₄ ⁺	5.58	3.16	15.97	1.81	4.02	3.17	15.05	0.91	21
K ₊	3.20	1.60	6.65	0.67	2.46	1.35	5.01	0.38	21
Na ₊	3.70	2.58	8.58	1.05	1.74	1.39	5.79	0.45	21
Ca ₂ ⁺	19.45	13.49	51.08	4.13	7.58	7.53	25.43	1.20	21
Mg ₂ ⁺	1.93	0.58	3.01	0.88	0.55	0.26	1.42	0.29	21
Cl ₋	1.85	1.15	4.99	0.22	0.98	0.76	2.93	0.10	21
OC	61.44	16.65	84.42	38.18	29.84	9.02	43.54	15.71	7

[Title Page](#)
[Abstract](#)
[Introduction](#)
[Conclusions](#)
[References](#)
[Tables](#)
[Figures](#)
[Back](#)
[Close](#)
[Full Screen / Esc](#)
[Printer-friendly Version](#)
[Interactive Discussion](#)

Observational study of aerosol hygroscopic growth factors

X. L. Pan et al.

Table 2. Designation of different dominant types of aerosol ($PM_{2.1}$).

Episode	Dominant aerosols	Wind direction/ Air mass pathway	$PM_{2.1}$ ($\mu\text{g}\cdot\text{m}^{-3}$)	$PM_{2.1}$ (%)	SO_4^{2-} ($\mu\text{g}\cdot\text{m}^{-3}$)	NO_3^- ($\mu\text{g}\cdot\text{m}^{-3}$)	NH_4^+ ($\mu\text{g}\cdot\text{m}^{-3}$)	Na^+	$f(RH=80\%)$	N
Dust	Dust particles	NW	128.22	18.50	6.11	3.13	1.82	0.78	1.20	2
Clean	Tiny fraction of Inorganic and organic matters	N	43.53	30.0	5.76	3.04	1.25	0.72	1.31	10
Urban	Urban anthropogenic aerosols	S/SE	87.93	42.8	13.14	7.12	4.63	1.62	1.57	37
Mixed	Urban and marine mixed	NE	81.80	65.2	4.32	1.21	1.84	5.79	2.24	1
		SE	86.14	39.5	9.26	2.78	4.14	2.55	2.21	3

Title Page

Abstract

Introduction

Conclusions

References

Tables

Figures

⏪

⏩

◀

▶

Back

Close

Full Screen / Esc

Printer-friendly Version

Interactive Discussion

Observational study of aerosol hygroscopic growth factors

X. L. Pan et al.

Title Page

Abstract

Introduction

Conclusions

References

Tables

Figures

◀

▶

◀

▶

Back

Close

Full Screen / Esc

Printer-friendly Version

Interactive Discussion



Table 3. Other observation results of hygroscopic growth factor of different types of aerosols.

Study region (Experiment)	Period	Aerosol type	$f(\text{RH}=80\%)^*$	RH range	References
Great Somky Mountain			1.95	82.8/40	
Grand Canyon	1995	rural	1.88	82.3/40	Day and Malm,
Big Bend			1.93	82.5/40	
Brazil (SCAR-B)	Aug–Sep 1995	Biomass burning	1.16(1.01~1.51)	80/30	Kotchenruther and Hobbs
Bondvillillionois	1995	Northern Hemisphere continental site (PM ₁₀)	1.42	82.5/40	Koloutsou-Vakakis et al.
		Polluted (PM ₁₀)	1.40		
Sagres, Portugal ACE-2	15 Jun–25 Jul 1997	Clean (PM ₁₀)	1.67	82.5/30	Carrico et al.
East Coast of US (TARFOX)	10–31 Jul 1996	Urban/industrial	1.81±0.37~2.30±0.24	80/30	Kotchenruther et al.
Cape Grim Tasmania ACE-1	15 Jun–25 Jul 1997	Rural	1.89	82.5/30	Carrico et al.
Yangtze delta	28 Oct–30 Nov 1999	Urban/background	1.7~2.0	85/40	Xu et al.
Southern Africa (SAFARI)	10 Aug–18 Sep 2000	Biomass burning	1.42±0.05~2.07±0.03	80/30	Magi and Hobbs
		Dust	1.69~1.73		
		Pollution (China)	2.0~2.43		
East Asia (ACE-Asia)	11–27 Apr 2001	Pollution (Korea)	1.55~1.77	85/40	Kim et al.
		Biomass burning	1.30~1.59		
		Pollution(PM ₁₀)	2.36		
East Asia (ACE-Asia)	Mar–Apr 2001	Marine(PM ₁₀)	2.04	85/35	Carrico et al.
		Dust (PM ₁₀)	1.25		
		Urban	2.04±0.28		
Pearl River Delta(PRD)	1–31 Jul 2006	Mixed	2.29±0.28	80/40	Liu et al.
		Marine	2.68±0.59		
SDZ regional Background monitoring station	Dec 2005	Clean	1.16	85/40	Yan et al.
		Urban pollution	1.34		
		Clean	1.27~1.34		
		Dust	1.17~1.23		
Jing-jin-tang (East Asia)	24 Apr–15 May 2006	Urban pollution	1.55~1.59	90/40	this study
		Mixed	2.33~2.48		

* Some values of $f(\text{RH}=80\%)$ are derived from the equations authors provided.

Observational study of aerosol hygroscopic growth factors

X. L. Pan et al.

Table 4. Curve-fitting parameters in different aerosol dominant episodes in terms of Eq. (2).

Classification	a	b	reference
dust	0.64±0.04	5.17±0.4	This work
clean	1.20±0.06	6.07±0.27	
urban	2.30±0.03	6.27±0.10	
mixed	7.68±0.15	7.62±0.14	
plume	0.18±0.02	6.11±0.43	Kotchenruther et al.
Regional haze	0.31±0.05	5.08±0.11	
urban	2.06	3.60	Liu et al.
mixed	3.26	3.85	
marine	4.92	5.04	

[Title Page](#)
[Abstract](#)
[Introduction](#)
[Conclusions](#)
[References](#)
[Tables](#)
[Figures](#)
[⏪](#)
[⏩](#)
[◀](#)
[▶](#)
[Back](#)
[Close](#)
[Full Screen / Esc](#)
[Printer-friendly Version](#)
[Interactive Discussion](#)

Observational study of aerosol hygroscopic growth factors

X. L. Pan et al.

Table 5. Relationship between the hygroscopic growth factor with chemical composition in $PM_{2.1}$.

date	$PM_{2.1}$ ($\mu\text{g}\cdot\text{m}^{-3}$)	$PM_{2.1}/PM_{1.1}$	SO_4^{2-} (%)	NH_4^+ (%)	NO_3^- (%)	OC (%)	AS ($\mu\text{g}\cdot\text{m}^{-3}$)	OMC ($\mu\text{g}\cdot\text{m}^{-3}$)	OMC/AS	$f(\text{RH}=80\%)$
05–03	107.63	45.79	15.27	3.84	7.64	29.77	20.67	44.85	0.46	1.51
05–04	178.21	50.32	17.68	3.82	9.37	24.43	38.57	60.96	0.63	1.56
05–10	42.05	29.02	11.24	2.15	5.24	37.37	5.67	22.00	0.26	1.13
05–11	81.80	42.13	5.29	2.25	1.48	40.02	6.14	45.83	0.13	2.24
05–12	102.81	57.52	9.47	3.80	5.68	26.03	13.62	37.46	0.36	1.50
05–13	42.67	27.05	6.07	4.45	1.24	36.66	4.44	21.90	0.20	1.26
05–14	49.78	34.19	8.86	3.82	1.06	39.37	6.29	27.44	0.23	1.21
05–15	86.14	39.49	10.75	4.81	3.23	43.00	13.35	51.86	0.26	2.21

Title Page

Abstract

Introduction

Conclusions

References

Tables

Figures

⏪

⏩

◀

▶

Back

Close

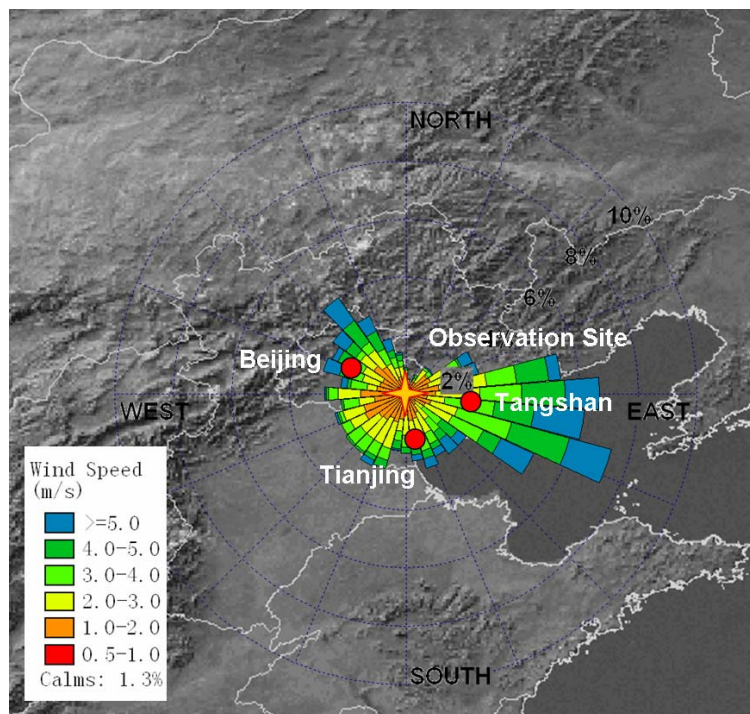
Full Screen / Esc

Printer-friendly Version

Interactive Discussion

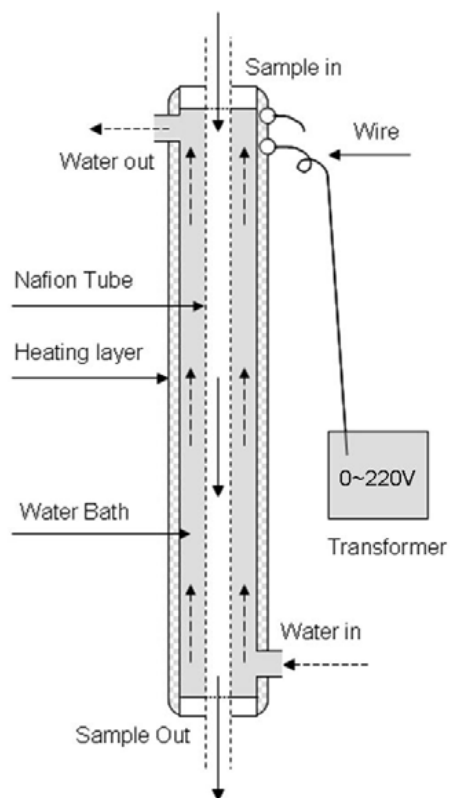
**Observational study
of aerosol
hygroscopic growth
factors**

X. L. Pan et al.

**Fig. 1.** Site Location and wind rose.[Title Page](#)[Abstract](#)[Introduction](#)[Conclusions](#)[References](#)[Tables](#)[Figures](#)[⏪](#)[⏩](#)[◀](#)[▶](#)[Back](#)[Close](#)[Full Screen / Esc](#)[Printer-friendly Version](#)[Interactive Discussion](#)

**Observational study
of aerosol
hygroscopic growth
factors**

X. L. Pan et al.

**Fig. 2.** Inlet relative humidity control device.[Title Page](#)[Abstract](#)[Introduction](#)[Conclusions](#)[References](#)[Tables](#)[Figures](#)[◀](#)[▶](#)[◀](#)[▶](#)[Back](#)[Close](#)[Full Screen / Esc](#)[Printer-friendly Version](#)[Interactive Discussion](#)

Observational study of aerosol hygroscopic growth factors

X. L. Pan et al.

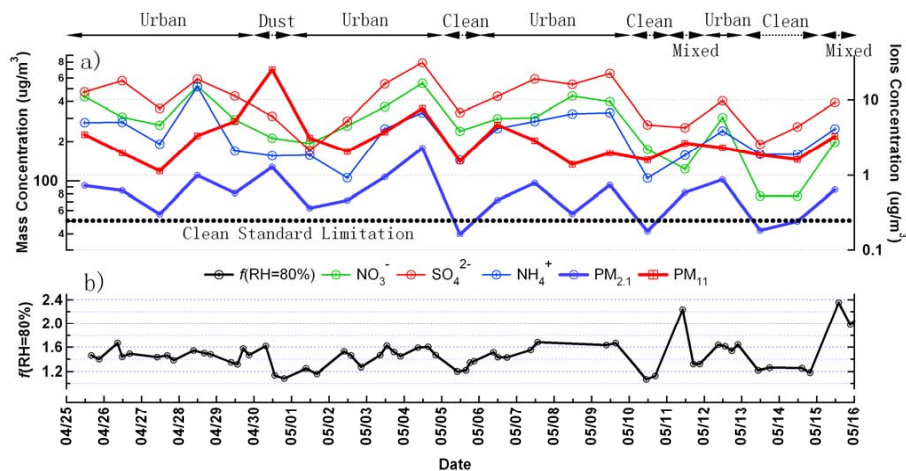


Fig. 3. Designation of different aerosol dominant episodes (a) Temporal variation of air mass concentration of $\text{PM}_{2.1}$ (thick blue line with solid dot) and PM_{11} (thick red line with solid dot) and chemical compositions in $\text{PM}_{2.1}$ (upper panel of the Fig. 3). (b) Temporal variation of hygroscopic growth factor $f(\text{RH}=80\%)$ during the whole observation periods.

Title Page

Abstract

Introduction

Conclusions

References

Tables

Figures

◀

▶

◀

▶

Back

Close

Full Screen / Esc

Printer-friendly Version

Interactive Discussion

**Observational study
of aerosol
hygroscopic growth
factors**

X. L. Pan et al.

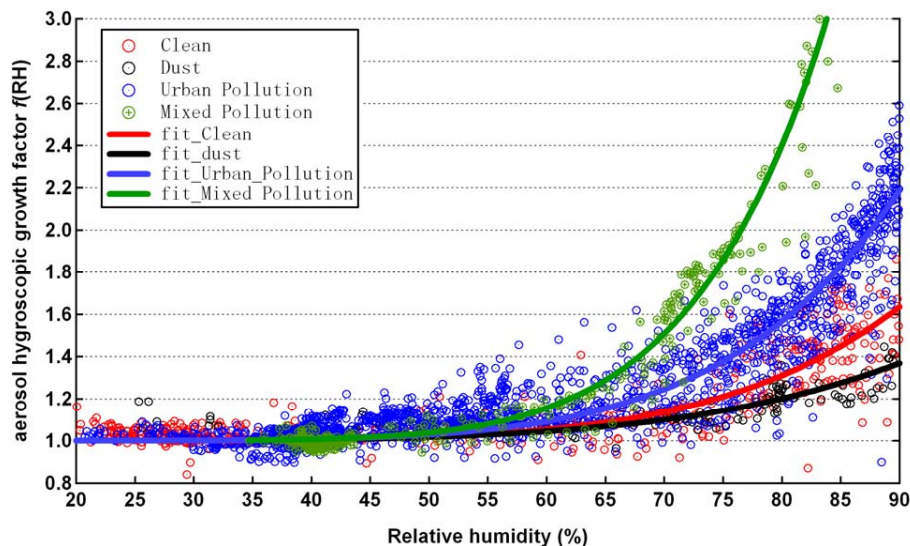


Fig. 4. Fitting curves of different dominant aerosol types. Among them, dot data represent the measurement results and lines stand for the fitting output of Eq. (2) for different aerosol types. Black, red, blue and green refer to the results of dust, clean, urban pollution and marine-urban mixed pollution episodes respectively.

[Title Page](#)[Abstract](#)[Introduction](#)[Conclusions](#)[References](#)[Tables](#)[Figures](#)[◀](#)[▶](#)[◀](#)[▶](#)[Back](#)[Close](#)[Full Screen / Esc](#)[Printer-friendly Version](#)[Interactive Discussion](#)

**Observational study
of aerosol
hygroscopic growth
factors**

X. L. Pan et al.

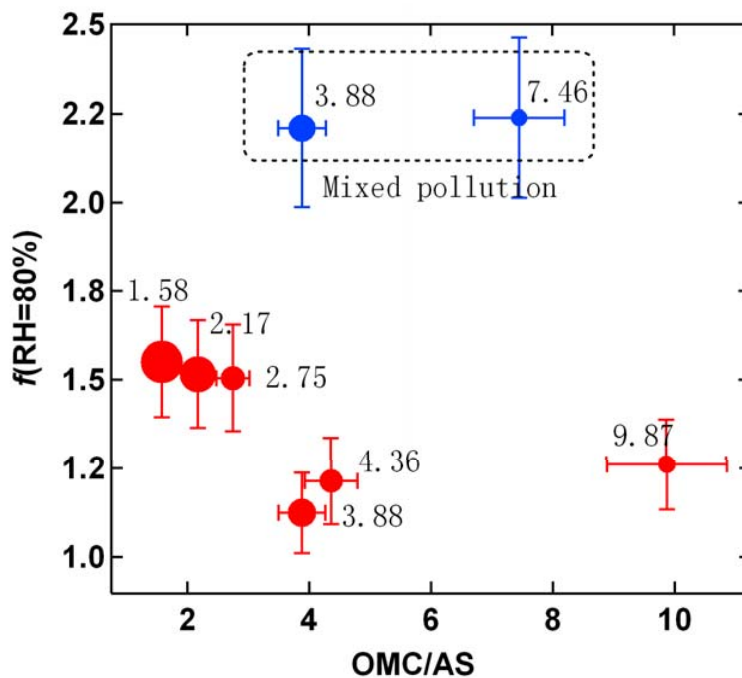


Fig. 5. Relationship between OMC/AS and $f(\text{RH}=80\%)$. With increasing ratio of OMC/AS, aerosol's hygroscopicity decline to some extent, except for the mixing pollution periods (show in blue dot).

[Title Page](#)[Abstract](#)[Introduction](#)[Conclusions](#)[References](#)[Tables](#)[Figures](#)[◀](#)[▶](#)[◀](#)[▶](#)[Back](#)[Close](#)[Full Screen / Esc](#)[Printer-friendly Version](#)[Interactive Discussion](#)

**Observational study
of aerosol
hygroscopic growth
factors**

X. L. Pan et al.

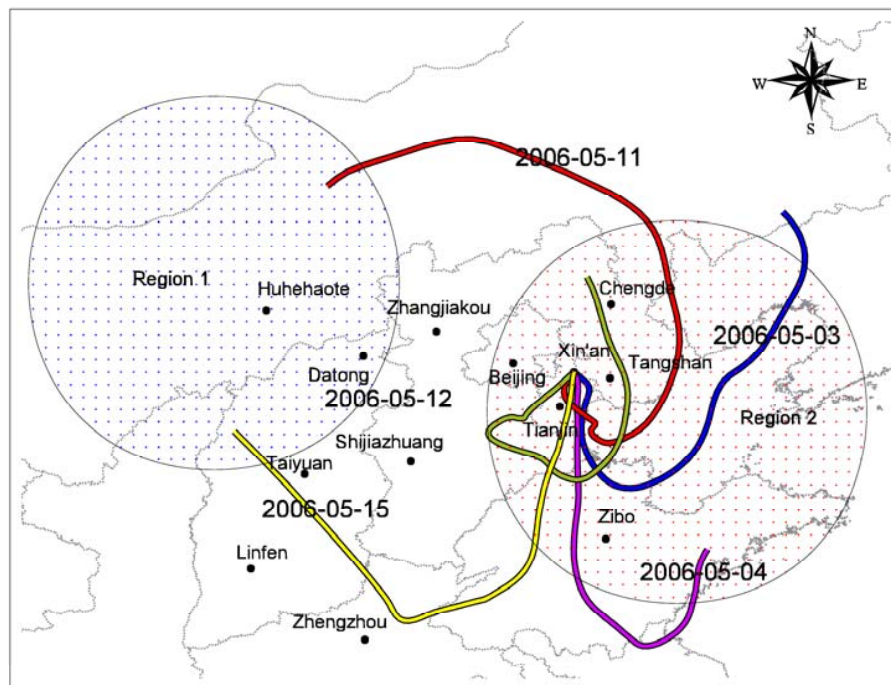


Fig. 6. The 48-h back trajectories of air masses during pollution episodes. The circles with blue dots (Region 1) and red dots (Region 2) stand for the possible contribution of aerosol type of source region on its corresponding hygroscopicity.

[Title Page](#)[Abstract](#)[Introduction](#)[Conclusions](#)[References](#)[Tables](#)[Figures](#)[◀](#)[▶](#)[◀](#)[▶](#)[Back](#)[Close](#)[Full Screen / Esc](#)[Printer-friendly Version](#)[Interactive Discussion](#)

**Observational study
of aerosol
hygroscopic growth
factors**

X. L. Pan et al.

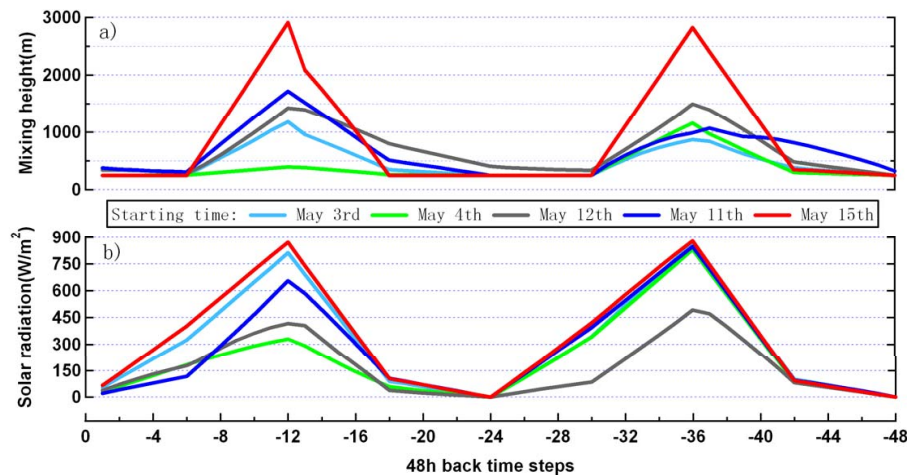


Fig. 7. The temporal variation of mixing height **(a)** and solar radiation **(b)** along the air pathway before arrived at Xin'An site. These data are from the outputs of Hysplit4 model.

[Title Page](#)[Abstract](#)[Introduction](#)[Conclusions](#)[References](#)[Tables](#)[Figures](#)[◀](#)[▶](#)[◀](#)[▶](#)[Back](#)[Close](#)[Full Screen / Esc](#)[Printer-friendly Version](#)[Interactive Discussion](#)